Available online at www.sciencedirect.com

ScienceDirect

IFAC PapersOnline CONFERENCE PAPER ARCHIVE

IFAC PapersOnLine 52-7 (2019) 57–62

Anisotropic heterogeneous n-D heat equation with boundary control and observation: II. Structure-preserving discretization ⋆

Anass Serhani * **Ghislain Haine** * **Denis Matignon** *

* *Institut Supérieur de l'Aéronautique et de l'Espace ISAE-SUPAERO, Université de Toulouse, 31055 TOULOUSE Cedex 4*

Abstract The heat equation with boundary control and observation can be described by means of three different Hamiltonians, the internal energy, the entropy, or a classical Lyapunov functional, as shown in the companion paper (Serhani et al. (2019a)). The aim of this work is to apply the partitioned finite element method (PFEM) proposed in Cardoso-Ribeiro et al. (2018) to the three associated port-Hamiltonian systems. Differential Algebraic Equations are obtained. The strategy proves very efficient to mimic the continuous Stokes-Dirac structure at the discrete level, and especially preserving the associated power balance. Anisotropic and heterogeneous 2D simulations are finally performed on the Lyapunov formulation to provide numerical evidence that this strategy proves very efficient for the accurate simulation of a boundary controlled and observed infinite-dimensional system.

Keywords: Port-Hamiltonian Differential Algebraic System, Heat Equation, Structure Preserving Discretization, Partitionned Finite Element Method (PFEM), Boundary Control

1. INTRODUCTION

The port-Hamiltonian formalism provides a powerful way to model complex systems, including laws coming from different realms. It is based on the use of physically meaningful quantities, linked through two kind of equations, namely physical laws and constitutive relations. The system it then obtained by interconnecting each domain (mechanics, thermodynamics, electromagnetism, etc.) through their ports, describing the exchange of energy between them. Furthermore, the physical parameters are intrinsically taken into account in the model, allowing for anisotropy and heterogeneity. This formalism highlights an underlying mathematical structure, namely (Stokes-)Dirac structure, that guarantees a balance equation for the Hamiltonian functional: the power balance. The Hamiltonian often describes the physical energy, but other type of functionals can be used.

A recent topic of research is to provide accurate discretization methods (both in time and space) to preserve this powerful formalism, and especially the power balance. Several strategies have been proposed to this aim, as mixed finite element/Galerkin in Golo et al. (2004); Kotyczka (2018); Kotyczka et al. (2018), finite difference in Trenchant et al. (2018), finite volume in Kotyczka (2016); Serhani et al. (2018). For time-domain discretization, Celledoni and Høiseth (2017) closely examine the question.

In view of these works, it seems that the partitionned finite element method (PFEM), first introduced in Cardoso-Ribeiro et al. (2018), is the most accurate way to proceed in space, as this work will try to prove.

PFEM relies on the fact that Hamiltonian systems in infinite dimension are used to formalize distributed parameters systems, hence including partial differential equations (PDE) given by physical laws. The idea is to write a variational formulation of the pHs, and integrate by parts only one of the equations of the weak form, accordingly with the desired control (it has to "appear" in the boundary term of the integration by parts). Then we use finite element to obtain a *finite dimensional* pHs, with accurate properties with respect to the infinite-dimensional one. PFEM has been succesfully used on various type of physical systems, such as acoustic pressure waves or plates in Brugnoli et al. (2019b,c); Serhani et al. (2019d).

In the following, the heat equation is considered in a bounded open connected set $\Omega \subset \mathbb{R}^n$, $n \geq 1$, with mass density $\rho(\mathbf{x})$, for all $\mathbf{x} \in \Omega$; $\overrightarrow{\mathbf{n}}$ denotes the outward unit normal. We suppose that this domain does not change over time, *i.e.* we work at *constant volume*. No chemical reactions are to be found in the domain. The quantities of interest are denoted as: u the internal energy density, $\overrightarrow{\mathbf{J}}_Q$ the heat flux, T the local temperature, $\beta := T^{-1}$ the reciprocal temperature, s the entropy density, $\overrightarrow{\mathbf{J}}_S := \beta \overrightarrow{\mathbf{J}}_Q$ the entropy flux, and $C_V := \left(\frac{\mathrm{d}u}{\mathrm{d}T}\right)_V$ the isochoric heat capacity.

⋆ This work has been performed in the frame of the Collaborative Research DFG and ANR project INFIDHEM n° ANR-16-CE92-0028 (http://websites.isae.fr/infidhem).

10.1016/j.ifacol.2019.07.010

In the companion paper Serhani et al. (2019a), the authors proposed to model the heat equation, controlled and observed at the boundary of the physical domain, by means of three different Hamiltonians. The first two are thermodynamically founded: the entropy and the internal energy, while the third one is less meaningful physically speaking, but enjoys an interesting behavior on a mathematical level. Reference to an equation (X) in this companion paper will be denoted by (I.X) in the present one.

We aim to apply the structure-preserving scheme PFEM to spatially discretize the three systems proposed in Serhani et al. (2019a) modeling the boundary controlled (and observed) heat equation. In the three cases, thermodynamical laws (*i.e.* constitutive relations) are needed to close the system. However, with the port-Hamiltonian formalism, the discretization of these relations can be postponed after the discretization of the physical laws. They need however to be carefully handled, suitably with the discretization of the port-Hamiltonian system.

The paper is organized as follows. In Section 2, PFEM is applied as a structure-preserving scheme on the three systems of Serhani et al. (2019a), and proves to be accurate for the corresponding Hamiltonians and its power balance. The Lyapunov case is then numerically experimented in Section 3 with 2D simulations to show the efficiency of the method, both on an isotropic and homogeneous case with analytically known solution and on an anisotropic and heterogeneous case. We end the paper with highlights and discussion about the pros and cons of PFEM compared to usual space discretizations.

2. A STRUCTURE-PRESERVING NUMERICAL METHOD: PFEM

This method is a recent structure-preserving method for pHs, first published in Cardoso-Ribeiro et al. (2018), and more recently developped in Cardoso-Ribeiro et al. (2019). The principle of the method lies on an integration by parts on a partition of the set of equations of the weak formulation of the continuous model, in order to make appear the control in the boundary integral.

Let us begin by a presentation of PFEM on the Lyapunov formulation. The method on the two other formulations will only be sketched, as most of the involved matrices will already be defined.

2.1 PFEM for the Lyapunov formulation

To begin with, let us write the weak formulation of (I.14). Denoting φ, $\overrightarrow{\boldsymbol{\varphi}}$ and ψ_∂ the test fonctions associated to f_u and e_u, $\overrightarrow{\boldsymbol{f}}_Q$ and $\overrightarrow{\boldsymbol{e}}_Q$, and v_∂ and y_∂ respectively, it reads

$$\begin{cases} \displaystyle\int_\Omega \rho f_u \varphi \,\mathrm{d}\mathbf{x} &= -\int_\Omega \operatorname{div}\left(\overrightarrow{\boldsymbol{e}}_Q\right)\varphi \,\mathrm{d}\mathbf{x}, \\ \displaystyle\int_\Omega \overrightarrow{\boldsymbol{f}}_Q \cdot \overrightarrow{\boldsymbol{\varphi}} \,\mathrm{d}\mathbf{x} &= -\int_\Omega \overrightarrow{\mathbf{grad}}\,(e_u)\cdot\overrightarrow{\boldsymbol{\varphi}} \,\mathrm{d}\mathbf{x}. \end{cases}$$

Integrating by parts the *first* line, one gets:

$$\begin{cases} \displaystyle\int_\Omega \rho f_u \varphi \,\mathrm{d}\mathbf{x} = \int_\Omega \overrightarrow{\boldsymbol{e}}_Q \cdot \overrightarrow{\mathbf{grad}}\,(\varphi) \,\mathrm{d}\mathbf{x} - \int_{\partial\Omega} \overrightarrow{\boldsymbol{e}}_Q \cdot \overrightarrow{\mathbf{n}}\varphi \,\mathrm{d}\gamma, \\ \displaystyle\int_\Omega \overrightarrow{\boldsymbol{f}}_Q \cdot \overrightarrow{\boldsymbol{\varphi}} \,\mathrm{d}\mathbf{x} = -\int_\Omega \overrightarrow{\mathbf{grad}}\,(e_u)\cdot\overrightarrow{\boldsymbol{\varphi}} \,\mathrm{d}\mathbf{x}, \end{cases} \tag{1}$$

leading to the choice of heat flux contol $v_\partial := -\overrightarrow{\boldsymbol{e}}_Q \cdot \overrightarrow{\mathbf{n}}_{|\partial\Omega}$.

Alternatively integrating by parts the *second* line

$$\begin{cases} \displaystyle\int_\Omega \rho f_u \varphi \,\mathrm{d}\mathbf{x} = -\int_\Omega \operatorname{div}\left(\overrightarrow{\boldsymbol{e}}_Q\right)\varphi \,\mathrm{d}\mathbf{x}, \\ \displaystyle\int_\Omega \overrightarrow{\boldsymbol{f}}_Q \cdot \overrightarrow{\boldsymbol{\varphi}} \,\mathrm{d}\mathbf{x} = \int_\Omega e_u \operatorname{div}\left(\overrightarrow{\boldsymbol{\varphi}}\right) \,\mathrm{d}\mathbf{x} - \int_{\partial\Omega} e_u \overrightarrow{\boldsymbol{\varphi}}\cdot\overrightarrow{\mathbf{n}} \,\mathrm{d}\gamma, \end{cases} \tag{2}$$

leads to the choice of temperature control $v_\partial := e_{u|\partial\Omega}$.

Assuming three *finite-dimensional* spaces

$$\begin{aligned} \mathcal{X} &:= \operatorname{span}\{\Phi\} := \operatorname{span}\{(\varphi^i)_{1\le i\le N}\}, \\ \boldsymbol{\mathcal{X}} &:= \operatorname{span}\{\overrightarrow{\boldsymbol{\Phi}}\} := \operatorname{span}\{(\overrightarrow{\boldsymbol{\varphi}}^k)_{1\le k\le \overrightarrow{\boldsymbol{N}}}\}, \\ \mathcal{X}_\partial &:= \operatorname{span}\{\Psi\} := \operatorname{span}\{(\psi_\partial^m)_{1\le m\le N_\partial}\}, \end{aligned}$$

one can define

$$f_{u,d}(t,\mathbf{x}) := \Phi^\top(\mathbf{x})\cdot \underline{f_u}(t) := \sum_{i=1}^{N} f_u^i(t)\varphi^i(\mathbf{x}) \simeq f_u(t,\mathbf{x}),$$

$$\overrightarrow{\boldsymbol{f}}_{Q,d}(t,\mathbf{x}) := \overrightarrow{\boldsymbol{\Phi}}^\top(\mathbf{x})\cdot \underline{f_Q}(t) := \sum_{k=1}^{\overrightarrow{\boldsymbol{N}}} f_Q^k(t)\overrightarrow{\boldsymbol{\varphi}}^k(\mathbf{x}) \simeq \overrightarrow{\boldsymbol{f}}_Q(t,\mathbf{x}),$$

and $v_{\partial,d}(t,\gamma) := \Psi^\top(\gamma)\cdot \underline{v_\partial}(t) := \sum_{m=1}^{N_\partial} v_\partial^m(t)\psi^m(\gamma) \simeq v_\partial(t,\gamma)$. Similarly, we define $e_{u,d}(t,\mathbf{x})$, $\overrightarrow{\boldsymbol{e}}_{Q,d}(t,\mathbf{x})$ and $y_{\partial,d}(t,\gamma)$ in $\mathcal{X}$, $\boldsymbol{\mathcal{X}}$, and $\mathcal{X}_\partial$ respectively.

The discrete weak formulation of (1) on $\mathcal{X}\times\boldsymbol{\mathcal{X}}\times\mathcal{X}_\partial$ reads

$$\begin{cases} M_\rho \underline{f_u}(t) &= D\underline{e_Q}(t) + B\underline{v_\partial}(t), \\ \overrightarrow{\boldsymbol{M}}\underline{f_Q}(t) &= -D^\top \underline{e_u}(t), \\ M_\partial \underline{y_\partial}(t) &= C\underline{e_u}(t), \end{cases} \tag{3}$$

with the following definitions

$$M_\rho := \int_\Omega \Phi\cdot\Phi^\top\rho \,\mathrm{d}\mathbf{x} \in \mathbb{R}^{N\times N},\quad \overrightarrow{\boldsymbol{M}} := \int_\Omega \overrightarrow{\boldsymbol{\Phi}}\cdot\overrightarrow{\boldsymbol{\Phi}}^\top \,\mathrm{d}\mathbf{x} \in \mathbb{R}^{\overrightarrow{\boldsymbol{N}}\times\overrightarrow{\boldsymbol{N}}},$$

$$M_\partial := \int_{\partial\Omega} \Psi\cdot\Psi^\top \,\mathrm{d}\gamma \in \mathbb{R}^{N_\partial\times N_\partial},$$

$$D := \int_\Omega \overrightarrow{\mathbf{grad}}\,(\Phi)\cdot\overrightarrow{\boldsymbol{\Phi}}^\top \,\mathrm{d}\mathbf{x} \in \mathbb{R}^{N\times\overrightarrow{\boldsymbol{N}}},$$

$$B := \int_{\partial\Omega} \Phi\cdot\Psi^\top \,\mathrm{d}\gamma \in \mathbb{R}^{N\times N_\partial},\quad C := \int_{\partial\Omega} \Psi\cdot\Phi^\top \,\mathrm{d}\gamma \in \mathbb{R}^{N_\partial\times N},$$

where $\overrightarrow{\mathbf{grad}}\,(\Phi)$ means the rectangular matrix of size $N\times n$, constituted of the gradient of each functions of Φ, *i.e.*

$$\overrightarrow{\mathbf{grad}}\,(\Phi) := \left(\left(\overrightarrow{\mathbf{grad}}\left(\varphi^1\right)\right)^\top,\ \cdots,\ \left(\overrightarrow{\mathbf{grad}}\left(\varphi^N\right)\right)^\top\right)^\top.$$

Note that the mass matrices M_ρ, $\overrightarrow{\boldsymbol{M}}$ and M_∂ are obviously symmetric. Furthermore, M_ρ discretizes the inner product of $L^2_\rho(\Omega)$. Finally, $C = B^\top$, hence (3) can be rewritten under the classical finite-dimensional pHs form, including the interconnection ports into the structure

$$\mathcal{M}_d \overrightarrow{\boldsymbol{f}}_d = \mathcal{J}_d \overrightarrow{\boldsymbol{e}}_d, \tag{4}$$

with $\mathcal{M}_d$ a symmetric matrix and $\mathcal{J}_d$ a skew-symmetric matrix, both of size $N + \overrightarrow{\boldsymbol{N}} + N_\partial$. More precisely

$$\overrightarrow{\boldsymbol{f}}_d := \left(\underline{f_u},\ \underline{f_Q},\ -\underline{y_\partial}\right)^\top,\quad \overrightarrow{\boldsymbol{e}}_d := \left(\underline{e_u},\ \underline{e_Q},\ \underline{v_\partial}\right)^\top,$$

$$\mathcal{M}_d := \begin{pmatrix} M_\rho & 0 & 0 \\ 0 & \overrightarrow{\boldsymbol{M}} & 0 \\ 0 & 0 & M_\partial \end{pmatrix},\quad \mathcal{J}_d := \begin{pmatrix} 0 & D & B \\ -D^\top & 0 & 0 \\ -B^\top & 0 & 0 \end{pmatrix}.$$

Note that the skew-symmetry of $\mathcal{J}_d$ and (4) imply

$$\overrightarrow{\boldsymbol{e}}_d^\top \mathcal{M}_d \overrightarrow{\boldsymbol{f}}_d = 0. \tag{5}$$

Now we want to define the discrete Hamiltonian and provide a discrete version of the balance equation (I.15).

Since $f_u(t,\mathbf{x}) := \partial_t u(t,\mathbf{x})$ in $L^2_\rho(\Omega)$, this leads to $\int_\Omega \rho(\mathbf{x}) f_u(t,\mathbf{x})\varphi(\mathbf{x})\,\mathrm{d}\mathbf{x} = \int_\Omega \rho(\mathbf{x})\partial_t u(t,\mathbf{x})\varphi(\mathbf{x})\,\mathrm{d}\mathbf{x}$. With the discrete family Φ, this becomes

$$M_\rho \underline{f_u}(t) = M_\rho d_t \underline{u}(t). \tag{6}$$

In the same way, $e_u := \frac{u(t,\mathbf{x})}{C_V(t,\mathbf{x})}$ in $L^2_\rho(\Omega)$ leads to

$$M_\rho \underline{e_u}(t) = M_{\rho C_V^{-1}}(t)\underline{u}(t), \tag{7}$$

where $M_{\rho C_V^{-1}}(t) := \int_\Omega \Phi\cdot\Phi^\top \frac{\rho}{C_V(t,\cdot)}\,\mathrm{d}\mathbf{x}$.

Denoting $u_d(t,\mathbf{x})$ the discrete counterpart of the internal energy density in $\mathcal{X}$, one can define the discrete Hamiltonian by $\mathcal{H}_d(t) := \frac{1}{2}\int_\Omega \rho(\mathbf{x})\frac{(u_d(t,\mathbf{x}))^2}{C_V(t,\mathbf{x})}\,\mathrm{d}\mathbf{x}$, leading to $\mathcal{H}_d(t) = \frac{1}{2}\underline{u}^\top(t) M_{\rho C_V^{-1}}(t)\underline{u}(t)$. Hence

$$d_t\mathcal{H}_d(t) = d_t\underline{u}^\top(t) M_{\rho C_V^{-1}}(t)\underline{u}(t) + \frac{1}{2}\underline{u}^\top(t) d_t M_{\rho C_V^{-1}}(t)\underline{u}(t).$$

From (6) and (7), one immediatly gets

$$d_t\mathcal{H}_d(t) = \underline{f_u}^\top(t) M_\rho \underline{e_u}(t) + \frac{1}{2}\underline{u}^\top(t) d_t M_{\rho C_V^{-1}}(t)\underline{u}(t).$$

Since $d_t M_{\rho C_V^{-1}}(t) = -M_{\rho C_V^{-1}}(t) d_t M^{-1}_{\rho C_V^{-1}}(t) M_{\rho C_V^{-1}}(t)$, and (7) gives $\underline{u}^\top(t) d_t M_{\rho C_V^{-1}}(t)\underline{u}(t) = -\underline{e_u}^\top(t) M_\rho d_t M^{-1}_{\rho C_V^{-1}}(t) M_\rho \underline{e_u}(t)$. The two above equalities and (5) lead to the discrete counterpart of (I.15):

$$\begin{aligned} d_t\mathcal{H}_d(t) = &-\underline{e_Q}^\top(t)\overrightarrow{\boldsymbol{M}}\underline{f_Q}(t) + \underline{v_\partial}^\top(t) M_\partial \underline{y_\partial}(t) \\ &- \frac{1}{2}\underline{e_u}^\top(t) M_\rho d_t M^{-1}_{\rho C_V^{-1}}(t) M_\rho \underline{e_u}(t). \end{aligned} \tag{8}$$

At this stage, constitutive relations have not been used. Assuming C_V to be time-invariant and $u = C_V T$, as in the Dulong-Petit model, leads in a weak sense to $\int_\Omega \rho(\mathbf{x})u(t,\mathbf{x})\varphi(\mathbf{x})\,\mathrm{d}\mathbf{x} = \int_\Omega \rho(\mathbf{x})C_V(\mathbf{x})T(t,\mathbf{x})\varphi(\mathbf{x})\,\mathrm{d}\mathbf{x}$, giving

$$M_\rho \underline{f_u}(t) = M_{\rho C_V}\, d_t \underline{T}(t), \tag{9}$$

where $M_{\rho C_V} := \int_\Omega \Phi\cdot\Phi^\top \rho C_V\,\mathrm{d}\mathbf{x}$. Of course, the definition of e_u given by (7) then simply becomes

$$M_\rho \underline{e_u}(t) = M_\rho \underline{T}(t). \tag{10}$$

Fourier's law (I.5) writes

$$\int_\Omega \overrightarrow{\mathbf{J}}_Q(t,\mathbf{x})\cdot\overrightarrow{\boldsymbol{\varphi}}(\mathbf{x})\,\mathrm{d}\mathbf{x} = -\int_\Omega \overline{\overline{\lambda}}(\mathbf{x})\cdot\overrightarrow{\mathbf{grad}}\,(T(t,\mathbf{x}))\cdot\overrightarrow{\boldsymbol{\varphi}}(\mathbf{x})\,\mathrm{d}\mathbf{x},$$

leading to

$$\overrightarrow{\boldsymbol{M}}\underline{e_Q}(t) = \overrightarrow{\boldsymbol{\Lambda}}\underline{f_Q}(t), \tag{11}$$

where $\overrightarrow{\boldsymbol{\Lambda}} := \int_\Omega \overrightarrow{\boldsymbol{\Phi}}\cdot\overline{\overline{\lambda}}\cdot\overrightarrow{\boldsymbol{\Phi}}^\top\,\mathrm{d}\mathbf{x} \in \mathbb{R}^{\overrightarrow{\boldsymbol{N}}\times\overrightarrow{\boldsymbol{N}}}$, which is symmetric by assumption on $\overline{\overline{\lambda}}$. Hence (8) becomes

$$d_t\mathcal{H}_d(t) = -\underline{f_Q}^\top(t)\overrightarrow{\boldsymbol{\Lambda}}\underline{f_Q}(t) + \underline{v_\partial}^\top(t) M_\partial \underline{y_\partial}(t), \tag{12}$$

the discrete counterpart of (I.16).

Following the same strategy, we obtain the discrete formulation of (2) in $\mathcal{X}\times\boldsymbol{\mathcal{X}}\times\mathcal{X}_\partial$

$$\begin{cases} M_\rho \underline{f_u}(t) &= \widetilde{D}\underline{e_Q}(t), \\ \overrightarrow{\boldsymbol{M}}\underline{f_Q}(t) &= -\widetilde{\overline{D}}^\top \underline{e_u}(t) + \widetilde{B}\underline{v_\partial}(t), \\ M_\partial \underline{y_\partial}(t) &= \widetilde{C}\underline{e_Q}(t), \end{cases} \tag{13}$$

with the following additional definitions

$$\widetilde{D} := -\int_\Omega \Phi\cdot\left(\mathrm{div}\left(\overrightarrow{\boldsymbol{\Phi}}\right)\right)^\top\,\mathrm{d}\mathbf{x} \in \mathbb{R}^{\overrightarrow{\boldsymbol{N}}\times N},$$

$$\widetilde{C}^\top := \widetilde{B} := -\int_{\partial\Omega}\left(\overrightarrow{\boldsymbol{\Phi}}\cdot\overrightarrow{\mathbf{n}}\right)\cdot\Psi^\top\,\mathrm{d}\gamma \in \mathbb{R}^{\overrightarrow{\boldsymbol{N}}\times N_\partial},$$

where $\mathrm{div}\left(\overrightarrow{\boldsymbol{\Phi}}\right)$ (resp. $\overrightarrow{\boldsymbol{\Phi}}\cdot\overrightarrow{\mathbf{n}}$) is the (column) vector of size $\overrightarrow{\boldsymbol{N}}$, constituted of the divergence (resp. the normal trace) of each functions of the family $\overrightarrow{\boldsymbol{\Phi}}$.

Note that it is again possible to write this system under the form (4), with $\widetilde{\mathcal{J}}_d := \begin{pmatrix} 0 & \widetilde{D} & 0 \\ -\widetilde{D}^\top & 0 & \widetilde{B} \\ 0 & -\widetilde{B}^\top & 0 \end{pmatrix}$.

2.2 PFEM for the energy formulation

Now the aim is to discretize the system related to the internal energy U as Hamiltonian, *i.e.* system (I.11). Its variational formulation reads

$$\begin{cases} \displaystyle\int_\Omega \rho f_s\varphi\,\mathrm{d}\mathbf{x} &= -\int_\Omega \mathrm{div}\left(\overrightarrow{\boldsymbol{e}}_S\right)\varphi\,\mathrm{d}\mathbf{x} - \int_\Omega e_\sigma\varphi\,\mathrm{d}\mathbf{x}, \\ \displaystyle\int_\Omega \overrightarrow{\boldsymbol{f}}_S\cdot\overrightarrow{\boldsymbol{\varphi}}\,\mathrm{d}\mathbf{x} &= -\int_\Omega \overrightarrow{\mathbf{grad}}\,(e_s)\cdot\overrightarrow{\boldsymbol{\varphi}}\,\mathrm{d}\mathbf{x}, \\ \displaystyle\int_\Omega f_\sigma\varphi\,\mathrm{d}\mathbf{x} &= \int_\Omega e_s\varphi\,\mathrm{d}\mathbf{x}. \end{cases}$$

Practically, it seems legitimate here to control the temperature, and thus integrate by parts the second line

$$\begin{cases} \displaystyle\int_\Omega \rho f_s\varphi\,\mathrm{d}\mathbf{x} &= -\int_\Omega \mathrm{div}\left(\overrightarrow{\boldsymbol{e}}_S\right)\varphi\,\mathrm{d}\mathbf{x} - \int_\Omega e_\sigma\varphi\,\mathrm{d}\mathbf{x}, \\ \displaystyle\int_\Omega \overrightarrow{\boldsymbol{f}}_S\cdot\overrightarrow{\boldsymbol{\varphi}}\,\mathrm{d}\mathbf{x} &= \int_\Omega e_s\cdot\mathrm{div}\left(\overrightarrow{\boldsymbol{\varphi}}\right)\,\mathrm{d}\mathbf{x} - \int_{\partial\Omega} e_s\overrightarrow{\boldsymbol{\varphi}}\cdot\overrightarrow{\mathbf{n}}\,\mathrm{d}\gamma, \\ \displaystyle\int_\Omega f_\sigma\varphi\,\mathrm{d}\mathbf{x} &= \int_\Omega e_s\varphi\,\mathrm{d}\mathbf{x}. \end{cases}$$

Following the same strategy as for the Lyapunov formulation, the following matrix form is computed

$$\begin{cases} M_\rho \underline{f_s}(t) &= \widetilde{D}\underline{e_S}(t) - M\underline{e_\sigma}(t), \\ \overrightarrow{\boldsymbol{M}}\underline{f_S}(t) &= -\widetilde{\overline{D}}^\top \underline{e_s}(t) + \widetilde{B}\underline{v_\partial}(t), \\ M\underline{f_\sigma}(t) &= M\underline{e_s}(t), \\ M_\partial \underline{y_\partial}(t) &= \widetilde{C}\underline{e_S}(t), \end{cases}$$

where

$$M := \int_\Omega \Phi\cdot\Phi^\top\,\mathrm{d}\mathbf{x} \in \mathbb{R}^{N\times N}. \tag{14}$$

The pHs form (4) then reads

$$\begin{pmatrix} M_\rho & 0 & 0 & 0 \\ 0 & \overrightarrow{\boldsymbol{M}} & 0 & 0 \\ 0 & 0 & M & 0 \\ 0 & 0 & 0 & M_\partial \end{pmatrix} \begin{pmatrix} \underline{f_s} \\ \underline{f_S} \\ \underline{f_\sigma} \\ -\underline{y_\partial} \end{pmatrix} = \begin{pmatrix} 0 & \widetilde{D} & -M & 0 \\ -\widetilde{D}^\top & 0 & 0 & \widetilde{B} \\ M & 0 & 0 & 0 \\ 0 & -\widetilde{B}^\top & 0 & 0 \end{pmatrix} \begin{pmatrix} \underline{e_s} \\ \underline{e_S} \\ \underline{e_\sigma} \\ \underline{v_\partial} \end{pmatrix}.$$

The discrete Hamiltonian is $U_d(t) := \int_\Omega \rho(\mathbf{x})u_d(t,\mathbf{x})\,\mathrm{d}\mathbf{x} = \underline{u}^\top(t) M_\rho \underline{\mathbf{1}}$, where $\underline{\mathbf{1}} \in \mathbb{R}^N$ is a vector full of ones.

The aim is to show that U_d enjoys a similar balance equation as U, *i.e.* similar to (I.13).

Gibbs formula (I.3) in a weak form reads

$$\int_\Omega \rho(\mathbf{x})\partial_t u(t,\mathbf{x})\,\mathrm{d}\mathbf{x} = \int_\Omega \rho(\mathbf{x})T(t,\mathbf{x})\partial_t s(t,\mathbf{x})\,\mathrm{d}\mathbf{x},$$

which gives at a discrete level with the pHs variables

$$d_t\underline{u}^\top(t) M_\rho \underline{\mathbf{1}} = \underline{f_s}^\top(t) M_\rho \underline{e_s}(t). \tag{15}$$

From the definition $\sigma := \overrightarrow{\mathbf{grad}}\,(\beta)\cdot\overrightarrow{\mathbf{J}}_Q$, one easily gets that $T\sigma = -\overrightarrow{\mathbf{grad}}\,(T)\cdot\overrightarrow{\mathbf{J}}_S$. This leads to

$$\int_\Omega T(t,\mathbf{x})\sigma(t,\mathbf{x})\,\mathrm{d}\mathbf{x} = -\int_\Omega \overrightarrow{\mathbf{grad}}\,(T(t,\mathbf{x}))\cdot\overrightarrow{\mathbf{J}}_S(t,\mathbf{x})\,\mathrm{d}\mathbf{x},$$

which then reads once discretized, in the pHs variables $-\underline{e_\sigma}^\top(t)M\underline{f_\sigma}(t) = \underline{e_S}^\top(t)\overrightarrow{\boldsymbol{M}}\underline{f_S}(t)$. This implies that (5) reduces to $\underline{e_s}^\top(t)M_\rho\underline{f_s}(t) = \underline{v_\partial}^\top(t)M_\partial\underline{y_\partial}(t)$. From (15), one gets the discrete counterpart of (I.13), namely:

$$d_t\mathcal{H}_d(t) = \underline{v_\partial}^\top(t)M_\partial\underline{y_\partial}(t).$$

To close the system, and be able to solve it, we need accurate constitutive relations, according to the physical system under study, as done in the Lyapunov case.

2.3 PFEM for the entropy formulation

Now, we discretize the system related to the entropy S as Hamiltonian, *i.e.* system (I.8). Practically, it seems legitimate here to control the boundary heat flux. In pHs variables, this is exactly the same system to discretize as for the Lyapunov formulation with boundary heat flux control. The difference lies in the definition of e_u and $\overrightarrow{\boldsymbol{f}}_Q$. Thus we have again system (13).

The discrete Hamiltonian is $S_d(t) := \int_\Omega \rho(\mathbf{x})s_d(t,\mathbf{x})\,\mathrm{d}\mathbf{x} = \underline{s}^\top(t)M_\rho\underline{\mathbf{1}}$. From Gibbs formula (I.3), as for (15), we get $d_t\underline{s}^\top(t)M_\rho\underline{\mathbf{1}} = \underline{f_u}^\top(t)M_\rho\underline{e_u}(t)$. From (5): $\underline{e_u}^\top(t)M_\rho\underline{f_u}(t) + \underline{e_Q}^\top(t)\overrightarrow{\boldsymbol{M}}\underline{f_Q}(t) = \underline{v_\partial}^\top(t)M_\partial\underline{y_\partial}(t)$. Finally, the definition $\sigma := \overrightarrow{\mathbf{grad}}(\beta)\cdot\overrightarrow{\mathbf{J}}_Q$ can be directly discretized by $\underline{\sigma}^\top(t)M\underline{\mathbf{1}} = -\underline{f_Q}^\top(t)\overrightarrow{\boldsymbol{M}}\underline{e_Q}(t)$. Hence the discretized counterpart of (I.9)

$$d_tS_d(t) = \underline{v_\partial}^\top(t)M_\partial\underline{y_\partial}(t) - \underline{f_Q}^\top(t)\overrightarrow{\boldsymbol{M}}\underline{e_Q}(t).$$

3. SIMULATION RESULTS

We now test PFEM on 2D examples. Simulations are performed on four cases: with heat flux boundary control or temperature boundary control, both for an isotropic homogeneous case where an analytical solution is known, and an anistropic heterogeneous case. We work with the Lyapunov Hamiltonian $\mathcal{H}$ under the hypotheses leading to (12). This choice was made as this is the usual "energy functional" in the applied mathematics literature.

The chosen geometry is the rectangle $\Omega := (0,2)\times(0,1)$. We propose to use $\mathbb{P}^2$ Lagrange finite element for Φ, RT^1 Raviart-Thomas finite element for $\overrightarrow{\boldsymbol{\Phi}}$ and $\mathbb{P}^2$ Lagrange finite element for Ψ. The corresponding degrees of freedom (Dof) are represented on Figure 1. This leads to $N = 204$ Dof for Φ, $\overrightarrow{\boldsymbol{N}} = 470$ Dof for Φ and $N_\partial = 50$ Dof for Ψ. The temperature T is approximated in the basis Φ. The discretization process will lead, either to an ordinary differential equation (ODE), or to a differential algebraic equation (DAE). To perform the simulations, we also need solvers to integrate in time these finite-dimensional differential equations. We use existing libraries to do it, without looking for time schemes which do not add numerical dissipation (as symplectic schemes for ODEs).

The simulations are carried out in Python 3, using FEniCS (Alnæs et al. (2015)) for the finite element libraries. The time integration for the ODEs is performed with the Runge-Kutta RK45 scheme, and with IDA (SUNDIALS) for DAEs. Note that the resolution of the DAE needs compatible initial data, which can be a drawback.

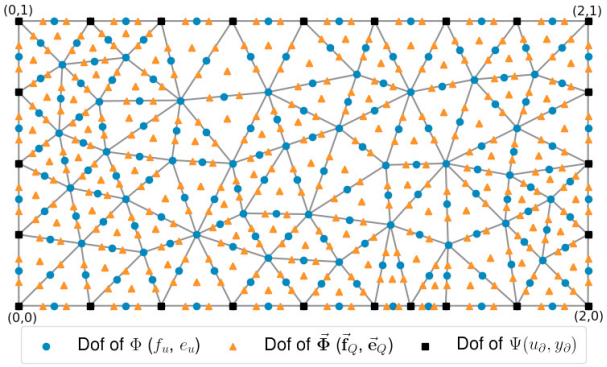

Figure 1. The used mesh, and the relative Dof.

3.1 Analytical solution

In this case, all the parameters are taken constant equal to one, *i.e.* $\rho = C_V \equiv 1$, $\overline{\overline{\lambda}} \equiv \begin{pmatrix}1 & 0\\ 0 & 1\end{pmatrix}$. Let $\mathbf{x} := \begin{pmatrix}x_1, & x_2\end{pmatrix}^\top$ and $T(t,\mathbf{x}) := 4t + \|\mathbf{x}\|^2 + 3x_1 - 5x_2$. Moreover, define $\overrightarrow{\mathbf{J}}_Q(t,\mathbf{x}) := -\overrightarrow{\mathbf{grad}}(T(t,\mathbf{x})) = -\begin{pmatrix}2x_1+3, & 2x_2-5\end{pmatrix}^\top$. It is clear that

$$\partial_tT(t,\mathbf{x}) = -\operatorname{div}\left(\overrightarrow{\mathbf{J}}_Q(t,\mathbf{x})\right) = \Delta T(t,\mathbf{x}), \quad \forall t\geq 0, \mathbf{x}\in\mathbb{R}^2.$$

Let us define the following function as boundary control:

$$v_\partial(t,\gamma) := \begin{cases} 5, & x_2 = 0,\\ 7, & x_1 = 2,\\ -3, & x_2 = 1,\\ -3, & x_1 = 0,\end{cases} \quad \forall t\geq 0,\ \gamma\in\partial\Omega. \tag{16}$$

Then T defined above is the solution of the following heat equation with boundary heat flux control

$$\begin{cases} \partial_tT(t,\mathbf{x}) = \Delta T(t,\mathbf{x}), & \forall t\geq 0, \mathbf{x}\in\Omega,\\ T(0,\mathbf{x}) = \|\mathbf{x}\|^2 + 3x_1 - 5x_2, & \forall \mathbf{x}\in\Omega,\\ \overrightarrow{\mathbf{grad}}(T(t,\gamma))\cdot\vec{\mathbf{n}}(\gamma) = v_\partial(t,\gamma), & \forall t\geq 0, \gamma\in\partial\Omega.\end{cases} \tag{17}$$

The associated observation is then given by

$$y_\partial(t,\gamma) = \begin{cases} 4t + x_1^2 + 3x_1, & x_2 = 0,\\ 4t + x_2^2 - 5x_2 + 10, & x_1 = 2,\\ 4t + x_1^2 + 3x_1 - 4, & x_2 = 1,\\ 4t + x_2^2 - 5x_2, & x_1 = 0,\end{cases} \quad \forall t\geq 0,\ \gamma\in\partial\Omega. \tag{18}$$

A straightforward computation gives $\mathcal{H}(t) = 16t^2 + \frac{52}{3}t + \frac{1301}{90}$. Hence $d_t\mathcal{H}(t) = 32t + \frac{52}{3}$. Also $\int_\Omega \left\|\overrightarrow{\mathbf{grad}}(T(t,\mathbf{x}))\right\|^2\,\mathrm{d}\mathbf{x} = \frac{256}{3}$, and $\int_{\partial\Omega} v_\partial(t,\gamma)y_\partial(t,\gamma)\,\mathrm{d}\gamma = 32t + \frac{320}{3}$, from which one verifies (I.16).

Boundary heat flux control Equation (17) is the prototype of linear parabolic PDE with Neumann boundary condition. Discretizing it by the finite element method is a classical exercise which can be found in any lecture notes on FEM. It only makes use of the family Φ. It gives rise to the following ordinary differential equation (ODE)

$$Md_t\underline{T}(t) = -A\underline{T}(t) + L(t), \quad \forall t\geq 0,$$

where M is defined in (14),

$$A := \int_\Omega \overrightarrow{\mathbf{grad}}(\Phi)\cdot\overrightarrow{\mathbf{grad}}(\Phi)^\top\,\mathrm{d}\mathbf{x} \in \mathbb{R}^{N\times N},$$

and $L(t) := \int_{\partial\Omega} v_\partial(t,\gamma)\Phi^\top(\gamma)\,\mathrm{d}\gamma \in \mathbb{R}^N$. This gives a first way to simulate T, called ODE-FEM in the sequel.

The second way is to solve the DAE constituted of (3)–(9)–(10)–(11). This method will be refer to as DAE-PFEM.

Finally, after substitutions, the above DAE leads also to the following ODE for the temperature

$$M_{\rho C_V}\, d_t \underline{T}(t) = -D\overrightarrow{\boldsymbol{M}}^{-1}\overrightarrow{\boldsymbol{\Lambda}}\overrightarrow{\boldsymbol{M}}^{-1}D^\top \underline{T}(t) + B\underline{v_\partial}(t),$$

i.e. using isotropy, homogeneity and the values given to the parameters: $M d_t \underline{T}(t) = -D\overrightarrow{\boldsymbol{M}}^{-1}D^\top \underline{T}(t) + B\underline{v_\partial}(t)$. We will refer to this method as ODE-PFEM.

Remark that in ODE-PFEM, the matrix $D\overrightarrow{\boldsymbol{M}}^{-1}D^\top$ is not sparse, contrarily to matrix A in ODE-FEM.

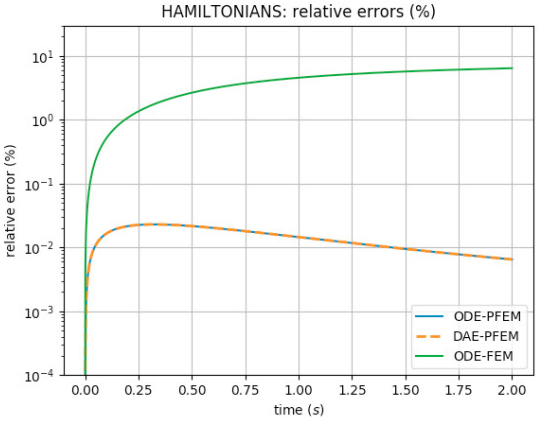

Figure 2. Relative errors between the discrete Hamiltonians and the analytical one (heat flux control).

One can appreciate on Figure 2 the efficiency of the two PFEM approaches, leading to a relative error of 10^{-4}, and still decreasing in time, whereas ODE-FEM seems to grow asymptotically to a relative error close to 10^{-1}.

Furthermore, it has to be noted that ODE-FEM and ODE-PFEM have the same size and are integrated in time with the same scheme. Thus, despite the non-sparsity of the finite element matrix $D\overrightarrow{\boldsymbol{M}}^{-1}D^\top$ leading to an overhead in CPU time and memory storage, there is still some interest in following this approach.

Boundary temperature control Now, the control v_∂ and the observation y_∂ respectively defined in (16) and (18) are switched, *i.e.* the heat equation is controlled by a prescribed temperature at the boundary of the domain (y_∂) and the heat flux is observed (u_∂).

The ODE-FEM approach has now a drawback, since the boundary temperature does not show up when integrating by part the weak formulation of (I.6). Thus, one needs a suitable scheme to impose the boundary control, such as lifting (time consuming since the control is time-dependent), or Lagrange multiplier. We use the latter in our simulations.

The DAE-PFEM approach only consists of solving the DAE constituted of (13)–(9)–(10)–(11), while substitutions allows again an ODE-PFEM approach

$$M d_t \underline{T}(t) = -\widetilde{D}\overrightarrow{\boldsymbol{M}}^{-1}\widetilde{D}^\top \underline{T}(t) + \widetilde{D}\overrightarrow{\boldsymbol{M}}^{-1}\widetilde{B}\underline{v_\partial}(t).$$

Figure 3 shows again the efficiency of PFEM, but only for the DAE resolution which gives a relative error at the computer precision. Remark that the error for ODE-PFEM, despite is value (10^{-13}) is not better than ODE-FEM. However, in long time, ODE-PFEM also reaches the computer precision while ODE-FEM stands still.

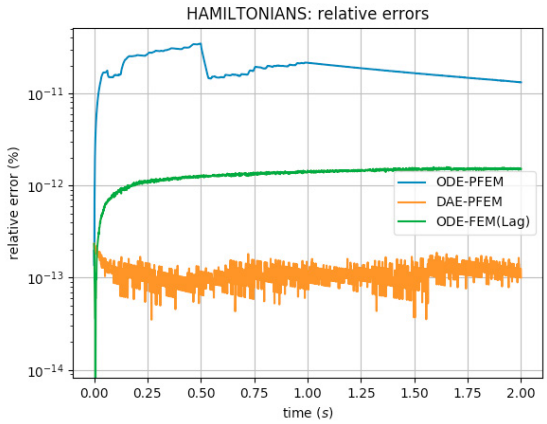

Figure 3. Relative errors between the discrete Hamiltonians and the analytical one (temperature control).

3.2 Anisotropic heterogeneous case

For this case, the parameters are taken to be

$$\rho(\mathbf{x}) := \mathbf{x}(2-\mathbf{x}) + 1,\ C_V := 3,\ \overline{\overline{\lambda}}(\mathbf{x}) := \begin{pmatrix} 5 + x_1 x_2 & (x_1 - x_2)^2 \\ (x_1 - x_2)^2 & 3 + \dfrac{x_2}{x_1 + 1} \end{pmatrix}.$$

The initial temperature is taken as a centered Gaussian, such that both temperature and heat flux are null at the boundary. Then a control is imposed either for the heat flux, or the temperature. It is taken to be under the form $v_\partial(t,\gamma) = f(t)g(\gamma)$, with $f(t) \sim \frac{t}{t+1}$ and $g(x_1, x_2) = x_1 + x_2$ at the boundary.

As an analytical solution would be difficult, not to say impossible, to compute, we compare the $L^2(\partial\Omega)$ relative error between the target control, and the effective value at the boundary of the approximation.

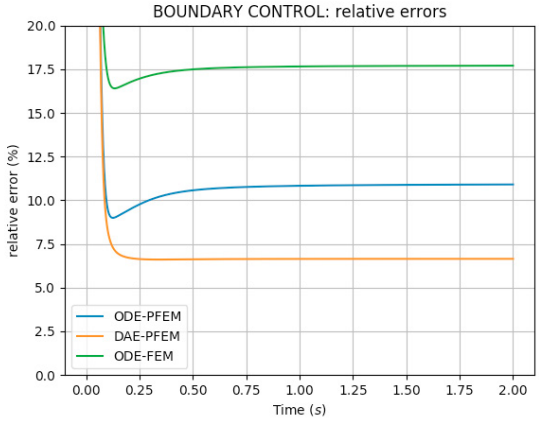

Figure 4. Relative errors in $L^2(\partial\Omega)$ between the target and effective boundary heat flux control.

Boundary heat flux control It can be seen on Figure 4, that DAE-PFEM has the best behavior. This can easily be explained. Since ODE-FEM and ODE-PFEM only approximates the temperature T, a post-processing is needed to compute the boundary heat flux, while it is directly accessible with DAE-PFEM.

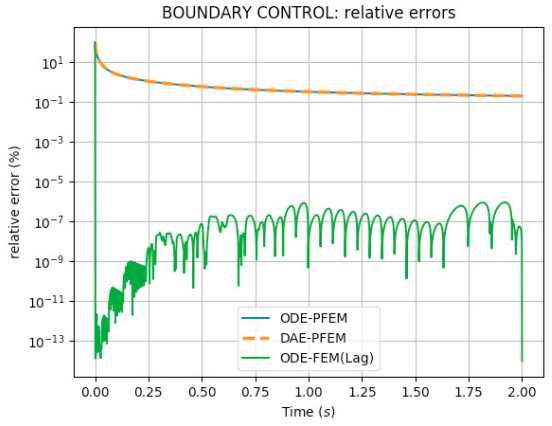

Figure 5. Relative errors in $L^2(\partial\Omega)$ between the target and effective boundary temperature control.

Boundary temperature control Figure 5 shows that the control is far better imposed with the classical Lagrange multiplier method. This can be explained by the fact that the Lagrange multiplier method strongly imposes the condition, while PFEM approaches weakly impose it.

4. CONCLUSION AND PERSPECTIVES

To conclude this paper, we summarize what has been done. The heat equation has been written in the pHs formalism, with three different Hamiltonian (Serhani et al. (2019a)). Two of them are thermodynamically founded, namely the entropy and the internal energy, and the third is a weighted L^2 norm, usually used in applied mathematic. PFEM has been applied on the obtained systems and it proves to be an accurate way to spatially discretize them, leading to finite-dimensional pHs. In particular, this leads to an accurate discretization of the chosen Hamiltonian. The main difficulty lies in the discretization of the constitutive relations, which has to be suitably adapted to the discretization of the flows and efforts. We finally perform simulations in 2D, under usual hypothesis (Fourier's law and time-invariant isochoric heat capacity) for the Lyapunov formulation. We show on the one hand, the efficiency of PFEM to simulate the system, first compared to an analytical solution in a simple case, and for an anisotropic heterogeneous case. On the other hand, we observed that solving directly the DAE system seems to be more relevant, although it involves a bigger system, and suitable time schemes.

Some numerical analysis should be made, as this is done in Serhani et al. (2019b) for the wave equation, leading to an optimal choice for the finite element families.

Furthermore, a deeper investigation of the theoretical relations between the finite-dimensional pHs and the continuous one would be of great benefit, in particular concerning the family of Dirac structures (as function of the mesh size parameter), for a better understanding of the underlying geometrical structures; see e.g. Serhani et al. (2019c).

REFERENCES

Alnæs, M., Blechta, J., Hake, J., Johansson, A., Kehlet, B., Logg, A., Richardson, C., Ring, J., Rognes, M., Wells, G., 2015. The FEniCS Project Version 1.5. Archive of Numerical Software 3 (100).

Brugnoli, A., Alazard, D., Pommier-Budinger, V., Matignon, D., 2019a. Partitioned finite element method for the Mindlin plate as a port-Hamiltonian system. In: 3rd IFAC workshop on Control of Systems Governed by Partial Differential Equations (CPDE).

Brugnoli, A., Alazard, D., Pommier-Budinger, V., Matignon, D., 2019b. Port-Hamiltonian formulation and symplectic discretization of plate models. Part I : Mindlin model for thick plates. Applied Mathematical Modelling. In press, arXiv:1809.11131.

Brugnoli, A., Alazard, D., Pommier-Budinger, V., Matignon, D., 2019c. Port-Hamiltonian formulation and symplectic discretization of plate models. Part II : Kirchhoff model for thin plates. Applied Mathematical Modelling. In press, arXiv:1809.11136.

Cardoso-Ribeiro, F. L., Matignon, D., Lefèvre, L., 2018. A structure-preserving partitioned finite element method for the 2D wave equation. IFAC-PapersOnLine 51 (3), 119–124.

Cardoso-Ribeiro, F. L., Matignon, D., Lefèvre, L., 2019. A partitioned finite-element method (PFEM) for power-preserving discretization of open systems of conservation laws. Submitted.

Celledoni, E., Høiseth, E., 2017. Energy-preserving and passivity-consistent numerical discretization of port-Hamiltonian systems. ArXiv:1706.08621.

Egger, H., Kugler, T., Liljegren-Sailer, B., Marheineke, N., Mehrmann, V., 2018. On structure-preserving model reduction for damped wave propagation in transport networks. SIAM Journal on Scientific Computing 40 (1), A331–A365.

Golo, G., Talasila, V., van der Schaft, A. J., Maschke, B., 2004. Hamiltonian discretization of boundary control systems. Automatica 40 (5), 757–771.

Hairer, E., Lubich, C., Wanner, G., 2006. Geometric numerical integration: structure-preserving algorithms for ordinary differential equations. Vol. 31. Springer Science & Business Media.

Kotyczka, P., 2016. Finite Volume Structure-Preserving Discretization of 1D Distributed-Parameter Port-Hamiltonian Systems. IFAC-PapersOnLine 49 (8), 298–303.

Kotyczka, P., July 16-20 2018. Structured discretization of the heat equation: Numerical properties and preservation of flatness. In: 23rd MTNS. Hong Kong.

Kotyczka, P., Maschke, B., Lefèvre, L., 2018. Weak form of Stokes–Dirac structures and geometric discretization of port-Hamiltonian systems. J. Computational Physics 361, 442–476.

Kunkel, P., Mehrmann, V., 2006. Differential-Algebraic Equations: Analysis and Numerical Solution. EMS Textbooks in Maths.

Leimkuhler, B., Reich, S., 2004. Simulating Hamiltonian dynamics. Vol. 14. Cambridge university press.

Serhani, A., Haine, G., Matignon, D., 2019a. Anisotropic heterogeneous n-D heat equation with boundary control and observation: I. Modeling as port-Hamiltonian system. In: 3rd IFAC workshop on Thermodynamical Foundation of Mathematical Systems Theory (TFMST). 6 p., These Proceedings.

Serhani, A., Haine, G., Matignon, D., 2019b. Numerical analysis of a semi-discretization scheme for the n-D wave equation in port-Hamiltonian system formalism. Submitted.

Serhani, A., Haine, G., Matignon, D., 2019c. A partitioned finite element method (PFEM) for the structure-preserving discretization of damped infinite-dimensional port-Hamiltonian systems with boundary control. In: Nielsen, F., Barbaresco, F. (Eds.), Geometric Science of Information 2019 (GSI'19). Lecture Notes in Computer Science. Springer, 10 p.

Serhani, A., Matignon, D., Haine, G., 2018. Structure-Preserving Finite Volume Method for 2D Linear and Non-Linear Port-Hamiltonian Systems. IFAC-PapersOnLine 51 (3), 131–136.

Serhani, A., Matignon, D., Haine, G., 2019d. Partitioned Finite Element Method for port-Hamiltonian systems with Boundary Damping: Anisotropic Heterogeneous 2-D wave equations. In: 3rd IFAC workshop on Control of Systems Governed by Partial Differential Equations (CPDE). 6 p., in press.

Trenchant, V., Ramirez, H., Gorrec, Y. L., Kotyczka, P., 2018. Finite differences on staggered grids preserving the port-Hamiltonian structure with application to an acoustic duct. J. Computational Physics 373, 673–697.